Biogeosciences, 9, 3231–3246, 2012
www.biogeosciences.net/9/3231/2012/
doi:10.5194/bg-9-3231-2012

Biogeosciences

Distributions of dissolved trace metals (Cd, Cu, Mn, Pb, Ag) in the southeastern Atlantic and the Southern Ocean

M. Boye[1], B. D. Wake[1,2], P. Lopez Garcia[2,3], J. Bown[1], A. R. Baker[4], and E. P. Achterberg[2]

[1]Institut Universitaire Européen de la Mer (IUEM) UMS3113, Laboratoire des Sciences de l'Environnement Marin UMR6539, Technopôle Brest Iroise, 29280 Plouzané, France
[2]School of Ocean & Earth Science, National Oceanography Centre Southampton, University of Southampton, Southampton SO14 3ZH, UK
[3]Universidad de Las Palmas de Gran Canaria, 35017 Las Palmas, Spain
[4]School of Environmental Sciences, University of East Anglia, Norwich, UK

Correspondence to: M. Boye (marie.boye@univ-brest.fr)

Received: 8 March 2012 – Published in Biogeosciences Discuss.: 21 March 2012
Revised: 12 July 2012 – Accepted: 14 July 2012 – Published: 23 August 2012

Abstract. Comprehensive synoptic datasets (surface water down to 4000 m) of dissolved cadmium (Cd), copper (Cu), manganese (Mn), lead (Pb) and silver (Ag) are presented along a section between 34° S and 57° S in the southeastern Atlantic Ocean and the Southern Ocean to the south off South Africa. The vertical distributions of Cu and Ag display nutrient-like profiles similar to silicic acid, and of Cd similar to phosphate. The distribution of Mn shows a subsurface maximum in the oxygen minimum zone, whereas Pb concentrations are rather invariable with depth. Dry deposition of aerosols is thought to be an important source of Pb to surface waters close to South Africa, and dry deposition and snowfall may have been significant sources of Cu and Mn at the higher latitudes. Furthermore, the advection of water masses enriched in trace metals following contact with continental margins appeared to be an important source of trace elements to the surface, intermediate and deep waters in the southeastern Atlantic Ocean and the Antarctic Circumpolar Current. Hydrothermal inputs may have formed a source of trace metals to the deep waters over the Bouvet Triple Junction ridge crest, as suggested by relatively enhanced dissolved Mn concentrations. The biological utilization of Cu and Ag was proportional to that of silicic acid across the section, suggesting that diatoms formed an important control over the removal of Cu and Ag from surface waters. However, uptake by dino- and nano-flagellates may have influenced the distribution of Cu and Ag in the surface waters of the subtropical Atlantic domain. Cadmium correlated strongly with phosphate (P), yielding lower Cd / P ratios in the subtropical surface waters where phosphate concentrations were below 0.95 µM. The greater depletion of Cd relative to P observed in the Weddell Gyre compared to the Antarctic Circumpolar Current could be due to increase Cd uptake induced by iron-limiting conditions in these high-nutrient–low-chlorophyll waters. Similarly, an increase of Mn uptake under Fe-depleted conditions may have caused the highest depletion of Mn relative to P in the surface waters of the Weddell Gyre. In addition, a cellular Mn-transport channel of Cd was possibly activated in the Weddell Gyre, which in turn may have yielded depletion of both Mn and Cd in these surface waters.

1 Introduction

Our understanding of the biogeochemical cycles of trace elements and their influence on the oceanic productivity in the high-nutrient–low-chlorophyll region of the Southern Ocean is still limited, with perhaps the exception of iron (Fe) (Martin et al., 1990; de Baar et al., 2005; Boyd et al., 2007). Certain trace metals have profiles that are nutrient-like, like cadmium (Cd) and copper (Cu), which is indicative of their involvement in biological cycles (Boyle, 1988; Boyle and Edmond, 1975). In contrast, other metals have a scavenged-type behavior like lead (Pb; Flegal and Patterson, 1983) or behave in a conservative manner like uranium (Bruland and Lohan, 2003). Elements such as manganese (Mn) can be considered

hybrid-type metals at high latitudes, as their distribution is controlled by both biological uptake and scavenging processes (Bruland and Lohan, 2003). Furthermore, the oceanic behavior of other trace metals like silver (Ag) is still not well understood, with little data on Ag distributions in the global ocean, notably in the Southern Hemisphere (Zhang et al., 2004). Despite major advances on the biological involvement of trace metals and their geochemical dynamics in the ocean, basic knowledge is still lacking on their biogeochemical cycles. For instance, there are only a few comprehensive datasets of Mn (Middag et al., 2011a), and of Cu, Cd and Pb (Löscher, 1999; Ellwood, 2008) for the Southern Ocean. The external sources of trace metals to the southeastern Atlantic and the Southern Ocean are not well constrained. Recent work suggests the importance of advection of water masses enriched in trace metals following contact with continental margins (Bown et al., 2011; Chever et al., 2010), in addition to atmospheric depositions to surface waters and inputs from hydrothermal vents to bottom waters (Middag et al., 2011a; Klunder et al., 2011). The coupling between trace and major nutrients cycles, such as the correlations between Cd and phosphate (PO_4) in the Southern Ocean (de Baar et al., 1994; Elderfield and Rickaby, 2000), indicates the removal of trace nutrients in surface waters due to phytoplankton uptake and their later sinking and remineralisation in deep waters. However, our knowledge of this coupling is still limited to a small number of trace elements. Such correlations have been used, alongside Cd / Ca ratios preserved in foraminifera tests, to reconstruct past changes in ocean circulation and nutrients distributions (Boyle, 1988). Furthermore, laboratory studies (Sunda and Huntsman, 2000) and shipboard incubation experiments (Cullen et al., 2003) have demonstrated the relationships between certain trace nutrients for phytoplankton uptake. For example, the depletion of Cd before that of PO_4 appears to be linked to Fe limitation in the Southern Ocean surface waters (Ellwood, 2008). Thus, a synoptic observation of trace nutrient distributions will increase our understanding of the coupling between the biogeochemical cycles of the trace nutrients in the Southern Ocean.

The emergence of new methods for trace metals analysis, such as isotope dilution-inductively coupled plasma mass spectrometry (ID-ICPMS) now allows us to achieve multi-element analyses with low limits of detection (Milne et al., 2010). The ID-ICPMS method has been employed here to further assess the biogeochemical cycles of Cd, Cu, Pb, Mn and Ag along a section in the southeastern Atlantic Ocean and the Southern Ocean south off South Africa during the International Polar Year in 2008. The survey area includes contrasting biogeochemical domains with the oligotrophic subtropical South Atlantic in the north, through to the high-nutrient–low-chlorophyll region of the Southern Ocean in the southern part of the section (Le Moigne et al., 2012). Furthermore, the section crosses one of the most dynamic and variable ocean domains in the world where the South Atlantic, Southern Ocean and Indian waters converge (Boebel et al., 2003). The distributions of the dissolved trace metals Cd, Cu, Mn, Pb, and Ag are discussed in combination with their atmospheric inputs, and the biogeochemical and physical features of the study region in order to determine the sources of these trace elements, their coupling with the major nutrients and the connection between their biogeochemical cycles.

2 Methods

2.1 Study area

Water samples were collected at twelve deep stations located in the southeast Atlantic and Atlantic sector of the Southern Ocean during the multidisciplinary MD 166 BONUS-GoodHope cruise. The cruise took place during the International Polar Year in the austral summer 2008 (8 February–24 March 2008) aboard the French *R/V Marion Dufresne II* (Fig. 1). The samples were collected from the shelf region off the South African coast to 57° S in the Weddell Gyre at the southern end of the section. The twelve stations consisted of seven LARGE stations (L#), sampled at up to ten depths to $\sim$ 2200 m, and five SUPER stations (S#), sampled at up to twenty depths to $\sim$ 4000 m. The station locations, oceanographic fronts and regions are marked on Fig. 1.

2.2 Sample collection

Samples were collected using acid-cleaned 12 l GO-FLO bottles (General Oceanics) modified with PTFE O-rings, mounted on a Kevlar wire and triggered using Teflon-coated messengers. The GO-FLO bottles were immediately transferred into a pressurized clean container (class 100) for subsampling. The samples were then collected in acid-cleaned 250 ml low-density polyethylene bottles (LDPE, Nalgene) after online filtration with a 0.22 µm Sartobran 300 (with 0.4 µM pre-filter, Sartorius) cartridge filter under pure N_2 pressure (filtered 99.99 % N_2, 1 bar). Each sample was then acidified to pH $\sim$ 1.9 on board in a laminar flow hood (class 100) with nitric acid (ultrapure $HNO_3^{®}$, Merck) and stored in double bags in the dark at ambient temperature until their analyses in the shore-based laboratory about 22 months after their collection.

2.3 Trace metal determination

Concentrations of dissolved trace metals (Cd, Pb, Cu) were determined by ID-ICPMS, and the mono-isotopic element Mn was analysed using a standard addition approach followed by ICPMS detection, following the methods described in Milne et al. (2010). The analysis was conducted following an offline preconcentration/matrix removal step on a Toyopearl AF-650M chelate resin column (Milne et al., 2010). Briefly, 15 ml of the acidified sample in an acid-cleaned 30 ml FEP bottle (Nalgene) was spiked with 100 µl of a multi-element standard of isotopes (containing the stable

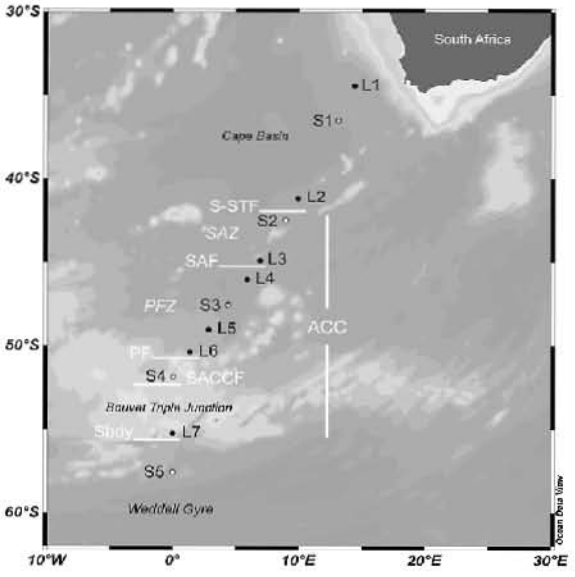

Fig. 1. Location of the stations sampled for dissolved Ag, Cd, Cu, Mn and Pb during the MD166 BONUS-GoodHope cruise. Black circles designate the LARGE stations (L) and white circles the SUPER stations (S). The positions of fronts are also shown, with the southern branch of the Subtropical Front (S-STF, $\sim 42°2'$ S), the Subantarctic Front (SAF, $44°2'$ S), the Polar Front (PF, $50°22.4'$ S), the Southern ACC Front (SACCF, $\sim 51°52'$ S) and the Southern Boundary of the ACC (Sbdy, $\sim 55°54.3'$ S). From their geographical positions, stations L1, S1 and L2 were in the Subtropical Zone (STZ), S2 was on the northern side of the Subantarctic Zone (SAZ), stations L3, L4, S3 and L5 were within the Polar Frontal Zone, station L6 was on the northern flank of PF, S4 was on the SACCF, station L7 was at the SBdy, and station S5 was in the northern branch of the Weddell Gyre. Figure prepared using Ocean Data View (Schlitzer, 2012).

isotopes ^{65}Cu, ^{111}Cd and ^{207}Pb; ISOFLEX, San Francisco, CA, USA) enriched over their natural abundance. A working solution of ^{65}Cu, ^{111}Cd and ^{207}Pb was prepared in 0.024 M ultrapure HNO_3 (Romil, Cambridge UK), and the exact concentration of the enriched isotope spikes in the mixed solution was determined by ICP optical emission spectroscopy (OES) against known natural standards (10 mg l^{-1}, ICP High Purity Standards) (Milne et al., 2010). Addition of the isotope spike to the sample contributed 60 pM Cd, 37 pM Pb and 1.13 nM Cu. In addition, standard additions of Mn were performed on sub-sets of the same seawater sample. The spiked samples were left for overnight equilibration. Subsequently, the samples were buffered to pH $\sim$ 6.2 using 2 M ammonium acetate, prepared with ultrapure acetic acid and ammonia (Romil, Cambridge, UK). The buffered sample was then pumped over the preconcentration column, at 2 ml min^{-1}. The column was rinsed with 1 ml de-ionised water to remove salts, and subsequently the metals were eluted using 1 ml of 1 M HNO_3 (Romil ultrapure HNO_3). The eluent was collected into acid cleaned autosampler polypropylene vials (OmniVials; 4 ml) and capped. Prior to loading of the next sample, the column was washed with an acid solution (1.5 M HCl) to remove residual trace elements. The extracted samples were analysed using a ThermoFisher Scientific Element II ICP-MS (E2 Bremen, Germany). The sample was introduced via a 100 µl Teflon nebuliser connected to a quartz spray chamber. Measurements for Cd and Pb were performed in low resolution mode ($R = 300$); whereas all other elements were measured in medium resolution ($R = 4000$).

Silver (Ag) was measured separately by ID-ICPMS with preconcentration on an anion-exchange column (Yang and Sturgeon, 2002; Barriada et al., 2007). In this method about 20 ml of the acidified sample was placed in an acid cleaned vial and spiked with ^{109}Ag stable isotope (75 µl of $\sim$ 5 nM solution in 0.024 M HNO_3 per 20 ml sample, 18.7 pM). The solution was allowed to equilibrate overnight. The sample was then pumped at 3 ml min^{-1} through a 1 cm long, 85 µM internal volume minicolumn (Global FIA, Inc., Fox Island, WA, USA) filled with a strong anion-exchange resin (Dowex 1X8, 200–400 mesh; Supelco, Bellefonte, CA, USA). The sample was eluted using 2 ml of 1.2 M HNO_3 (Romil SpA). Measurements were performed using an X-SERIES 2 ICP-MS (Thermo Fisher Scientific, Bremen, Germany) in the standard configuration, interfaced with an ASX-510 autosampler (Cetac, Omaha, Nebraska, USA). The concentration of the ^{109}Ag spike solution was determined using ICP-OES.

The accuracy and precision of the methods were assessed by analyses of SAFe (Sampling and Analysis of iron) and GEOTRACES reference samples (http://www.geotraces.org/science/intercalibration/322-standards-and-reference-materials), and results are reported in Table 1. The values determined using the ID-ICPMS method show good consistency with the reported consensus values for dissolved Cd and Pb (Table 1). There is no consensus value for dissolved Ag yet, hence the data recorded in this work may provide a basis for later analyses of the reference samples. Dissolved Cu concentrations determined by ID-ICPMS were lower compared to the consensus values, especially in the deep samples (Table 1), possibly because the samples were not exposed to UV-irradiation prior their analyses (Milne et al., 2010). Dissolved Mn detected by ICPMS yielded higher concentrations than the consensus values (Table 1), in line with the general trend that shows higher dissolved Mn concentrations using methods based upon ICP-MS as compared to those based upon catalytic-enhanced flow injection (http://www.geotraces.org/images/stories/documents/intercalibration/Files/Reference_Samples_November11/SAFe_Ref_Mn.pdf).

The complete database of the dissolved concentrations of Cd, Cu, Mn, Ag and Pb at the stations LARGE and SUPER can be obtained via http://www.obs-vlfr.fr/proof/php/x_datalist.php?xxop=bonusgh&xxcamp=bonusgh, and will be available at the international GEOTRACES datacenter (http://www.bodc.ac.uk/geotraces/).

Table 1. Comparison of dissolved Cd, Cu, Pb and Ag analyses obtained in the present study by the ID-ICPMS method and of dissolved Mn obtained by the internal standard addition and ICPMS detection, with the consensus values reported by the SAFe project (in the surface-S and deep-D2 samples) and in the North Atlantic GEOTRACES (in the surface-GS and deep-GD samples) Reference Samples (updated in November 2011). All ± terms represent standard deviation from average values.

	SAFe concentration		Consensus value SAFe		GEOTRACES concentration		Consensus value GEOTRACES	
	S	D2	S	D2	GS	GD	GS	GD
Cd	0.77 ± 0.96 pM ($n = 4$)	1034 ± 15 pM ($n = 8$)	1.00 ± 0.2 pM	986 ± 27 pM	2.86 ± 0.37 pM ($n = 3$)	287 ± 7 pM ($n = 4$)	2.4 ± 0.4 pM	273 ± 6 pM
Cu	0.56 ± 0.03 nM ($n = 10$)	1.39 ± 0.13 nM[a] ($n = 9$)	0.51 ± 0.05 nM	2.25 ± 0.11 nM	0.72 ± 0.07 nM[a] ($n = 4$)	1.12 ± 0.04 nM[a] ($n = 4$)	0.83 ± 0.08 nM	1.55 ± 0.13 nM
Mn	0.93 ± 0.06 nM ($n = 4$)	0.49 ± 0.07 nM ($n = 4$)	0.79 ± 0.06 nM[b]	0.35 ± 0.06 nM[b]	Not measured	Not measured	1.45 ± 0.17 nM	0.21 ± 0.04 nM
Pb	51.2 ± 2.2 pM ($n = 11$)	36.3 ± 1.4 pM ($n = 7$)	47.6 ± 2.4 pM	27.7 ± 1.8 pM	31.1 ± 1.6 pM ($n = 4$)	43.8 ± 3.2 pM ($n = 4$)	29.5 ± 2.1 pM	42.2 ± 1.3 pM
Ag	3.5 ± 0.7 pM ($n = 3$)	26.2 ± 0.9 pM ($n = 5$)	No value	No value	2.7 ± 0.9 pM ($n = 3$)	13.1 ± 1.0 pM ($n = 4$)	No value	No value

[a] The UV oxidation of the samples might be required to obtain an accurate value for dissolved Cu using this method (Milne et al., 2010).
[b] In general, methods based upon ICP-MS yield higher dissolved Mn concentrations than methods based upon catalytic-enhanced flow injection. Furthermore, there are significant differences between UV treatment and non-UV treated samples for dissolved Mn
http://www.geotraces.org/images/stories/documents/intercalibration/Files/Reference_Samples_November11/SAFe_Ref_Mn.pdf.

2.4 Aerosol sampling and analysis

Aerosol samples were collected onto single 20×25 cm Whatman 41 filters using a Tisch TSP high volume aerosol collector operating at a flow rate of $\sim 1\,m^3\,min^{-1}$ (Baker et al., 2007). Due to the very low aerosol concentrations in the study region, collection times for each sample were relatively long (2–3 days), and the collector was only used when the ship was heading into the prevailing wind in order to avoid contamination from the ship. Collection filters were extensively acid-washed before use, with 0.5 M Aristar HCl, 0.1 M Aristar HCl (Rickli et al, 2010), followed by a further wash with 0.1 M Suprapure HCl, which was carried out in a trace metal clean laboratory.

After collection, samples were sealed in plastic bags and immediately frozen at −16 °C for return to the shore laboratory. One quarter of each aerosol filter was extracted into 1 M ammonium acetate solution for between 1 and 2 h and the solution filtered through 0.2 µM minisart filters (Sartorius), as described in Baker et al. (2007). Soluble Mn, Cu, Pb, Cd and Ag were then determined by ICP-OES (Mn and Cu) and ICP-MS (Pb, Cd, Ag). Concentrations of Cd and Ag were below analytical detection limits (0.05–0.2 pmol m^{-3}) in all cases. Concentrations ranges for the other elements were 0.8–4.8 pmol m^{-3} (Mn), 4.3–13 pmol m^{-3} (Cu) and 0.27–0.83 pmol m^{-3} (Pb). Here we estimate the dry deposition flux of these elements as the product of their aerosol concentrations and a dry deposition velocity. We used an estimated dry deposition velocity of 0.3 cm s^{-1}, a value appropriate for elements likely to be chiefly associated with fine mode aerosol (Duce et al., 1991). We emphasize that dry deposition velocities are probably uncertain to plus or minus a factor of 2–3 (Duce et al., 1991), hence our calculated dry fluxes should be considered as order of magnitude estimates.

Atmospheric deposition of trace metals is also likely to occur through wet deposition. Attempts to sample rain and snow during the cruise were unsuccessful and we are therefore unable to make direct estimates of the magnitude of this wet flux. However, the northern part of the transect is relatively dry (Xie and Arkin, 1997) and wet deposition likely makes a less significant contribution there than in the south (Baker et al., 2010).

3 Results

3.1 Hydrography

A comprehensive description of the hydrography along the meridional section of this voyage is given in Bown et al. (2011). Further details are provided for the 2004 occupation of this CLIVAR GoodHope Line in Gladyshev et al. (2008). Briefly, the Subtropical Zone (STZ) extended to the southern branch of the Subtropical Front (S-STF; ∼ 42° S), including stations L1, S1 and L2 (Fig. 1). Despite its geographical location, S2 exhibited *S* and *T* signatures of subtropical waters (Bown et al., 2011), and this station will be discussed within the subtropical domain. The subtropical domain in the Cape Basin region is characterized by a very complex dynamic regime (Lutjeharms and Vanballegooyen, 1988; Gordon et al., 1992). The central water layer was mainly occupied by waters of Indian origin (Gordon et al., 1992). Antarctic Intermediate Water of Indian Ocean origin (I-AAIW) was observed at depths between 800 and 1200 m in the region close to Africa (stations L1 and S1), whereas another variety of AAIW was observed to the south (at L2 and S2) featuring AAIW formed in the subantarctic region of the southwest Atlantic (A-AAIW; Piola

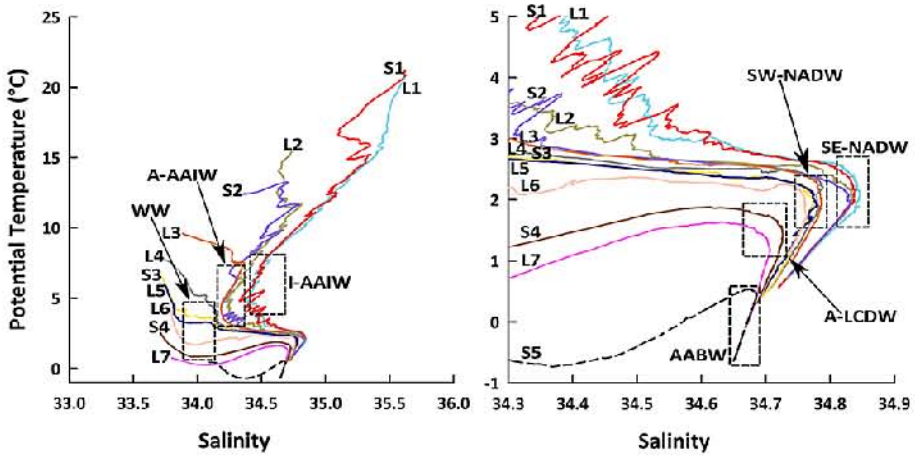

Fig. 2. Diagrams of potential temperature (°C) versus salinity in the whole water column (left panel) and in deep waters (right panel) at the stations sampled for trace metals determination (CTD data and validation from Branellec et al., 2010; Kermabon and Arhan, 2008).

and Gordon, 1989) (Fig. 2). The Upper Circumpolar Deep Water was found at a depth range of ∼1200–1500 m, and characterized by its oxygen minimum (160–180 µmol kg^{-1}). The complex water mass structure observed at L1 and S1 was likely transported by the Agulhas Current and rings, whereas it may originate from the southwest Atlantic (A-UCDW) at L2 and S2. At greater depths, a diluted variety of the North Atlantic Deep Water was observed which was transported along the southwest African continental shelf (SE-NADW; Arhan et al., 2003; Gladyshev et al., 2008) and characterised by its S signature (Fig. 2) and an oxygen maximum at 2000–3200 m depth at S1 and S2. Near the seafloor an old variety of Antarctic Bottom Water (AABW) was observed in the Cape Basin abyssal plain at S1. In the Antarctic Circumpolar Current (ACC; Fig. 1), the surface water was marked by a southward decrease of temperature from 4 °C (L5) to 2 °C (S4) and low *S* (Fig. 2). Below the surface mixed layer, A-AAIW was observed; this water mass subducted northward along the Subantarctic Front (SAF). At greater depths the Antarctic Winter Waters (AAWW; characterized by a *T* minimum; Fig. 2), the A-UCDW, and a diluted variety of NADW which flows along the continental slope of South America before being injected in the ACC in the southwestern Atlantic (SW-NADW; Whitworth and Nowlin, 1987) were observed north of the Polar Front (PF). South of the PF, another variety of UCDW which had passed through the Drake Passage (DP-UCDW) was identified by a core of low oxygen water (stations L6, S4 and L7). There deep waters exhibited properties of Lower Circumpolar Deep Waters (LCDW; Fig. 2). Finally, south of the Southern Boundary of the ACC (SBdy), the near surface waters may have been in contact with the western continental margin of the Antarctic Peninsula, while the deeper waters may have been in contact with the northern topographic limit of the Weddell Basin (Orsi et al., 1993; Meredith et al., 2000). Near the seafloor a fresher and colder variety of AABW was observed south of the ACC domain, as compared to AABW observed in the Cape Basin abyssal plain and on the northern flank of the Mid-Atlantic Ridge (Fig. 2).

3.2 Dissolved copper

The vertical distributions of dissolved Cu displayed nutrient-like behavior with lower concentrations in surface waters and increasing levels with depth (Figs. 3 and 4). There was a clear north–south gradient in the ACC and the Weddell Gyre waters, with the southern waters having higher concentrations compared to the north of the area (Fig. 3). This gradient followed that of silicate (Fig. 4). The highest Cu concentrations in surface waters were recorded in the northern branch of the Weddell Gyre (Fig. 3). In contrast, in the subtropical waters the dissolved Cu concentrations decreased in southward direction, and were lowest in the south of this domain (at stations L2 and S2) where enhanced chlorophyll *a* concentrations were observed along the section (Le Moigne et al., 2012). Deep maxima of Cu were observed in the cores of I-AAIW and SE-NADW (at S1), A-AAIW (at L3, L4 and L5), A-UCDW (at L3), and DP-UCDW (at S4) (Figs. 3 and 4).

3.3 Dissolved silver

Vertical distributions of dissolved Ag generally showed lower concentrations in surface waters and increasing concentrations with depth (Fig. 3), similar to silicate (Fig. 4). There was a general north–south trend in the Ag concentrations along the section, with the concentrations of Ag being generally lower in the subtropical domain than in the ACC (Fig. 3). Relative Ag minima were observed at several stations at depths between 150 and 350 m (Figs. 3 and 4) coinciding with oxygen minima (see dissolved O_2 profiles in Bown et al., 2011), whereas relative maxima were recorded

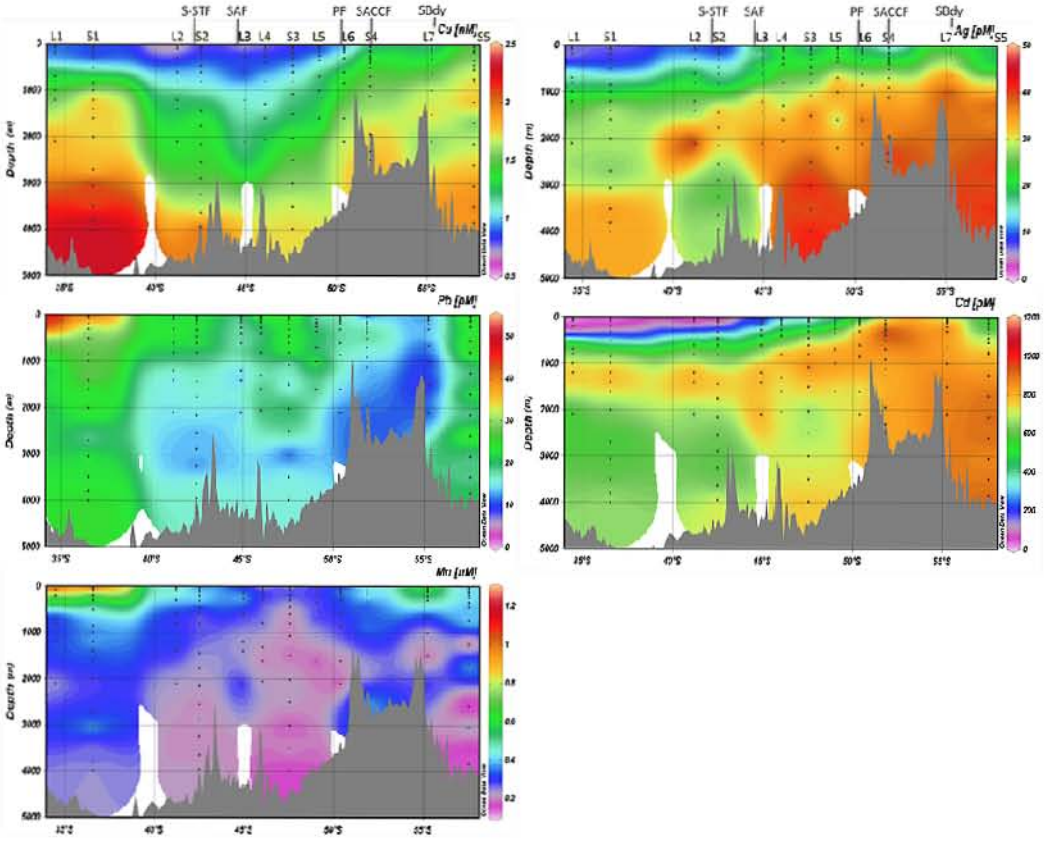

Fig. 3. Contour plots of dissolved copper (Cu, in nM), silver (Ag, in pM), lead (Pb, in pM), cadmium (Cd, in pM) and manganese (Mn, in nM) along the MD166 BONUS-GoodHope section between the southeastern Atlantic and the Southern Ocean. The positions of L and S stations and the fronts are indicated. The colour map gridding is based on the sampling resolution along the section of ∼2600 km that was achieved with 12 stations separated on average by ∼2.2° latitude, with a total of 160 sampling depths. Figure prepared using Ocean Data View (Schlitzer, 2012).

in deeper waters in the cores of the different varieties of UCDW – UCDW which was transported by the Agulhas Current (at S1), of southwest Atlantic origin (at S2), and which had passed through the Drake Passage (at S4 and L7). Conversely, Ag was relatively depleted in the cores of SE-NADW (at S1 and S2) and SW-NADW (L3 to L5).

3.4 Dissolved lead

The distributions of Pb were rather constant with depth across the section (with concentrations ranging between 10.2 and 32.3 pM), with the exception of the two northern stations closest to South Africa (L1 and S1) where Pb concentrations were much higher in the top 100 m depth (e.g. 37–55 pM) than in deeper waters (Fig. 3). Enrichment in the core of I-AAIW was observed at S1 station (Fig. 3). The lowest concentrations of Pb at depth (7.1–12.0 pM) were observed at the Southern Boundary of the ACC (station L7; Fig. 3).

3.5 Dissolved cadmium

Dissolved Cd concentrations increased markedly with depth (Fig. 3), similar to the major nutrient phosphate (Fig. 4). There was an obvious north–south gradient in the surface concentrations of Cd, similar to phosphate (Fig. 4), with lower concentrations in the northern waters (as low as 3.8 pM) as compared to much higher Cd concentrations in the southern waters of up to 895 pM at the ACC Southern Boundary (Figs. 3 and 4). However, the surface Cd concentrations in the Weddell Gyre were different from this pattern, since they were generally lower than the values recorded on the southern side of the ACC, south of the PF (Fig. 3).

3.6 Dissolved manganese

The vertical distributions of dissolved Mn generally showed low concentration in surface waters, a subsurface maximum in the oxygen minimum zone deepening southwards, and rather constant and low deep water concentrations in the range of or below the surface values (Figs. 3 and 4).

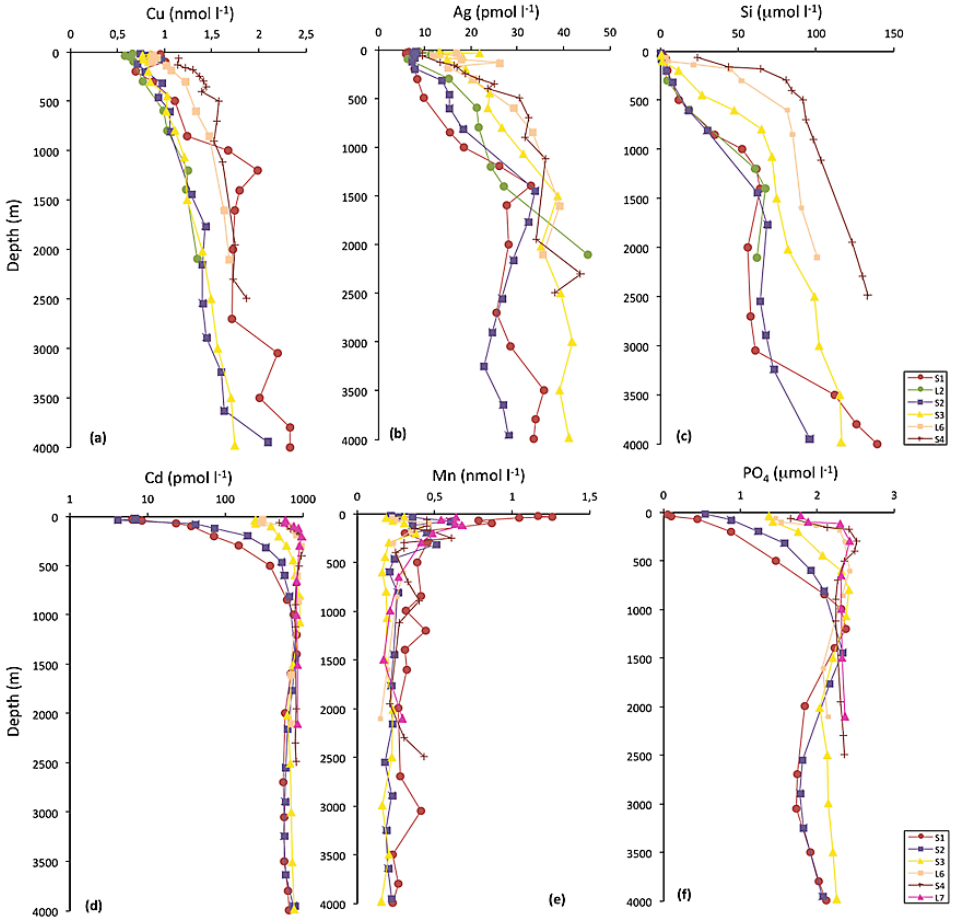

Fig. 4. Vertical distributions of dissolved copper **(a)** and silver **(b)**, silicic acid **(c)**, dissolved cadmium **(d)**, manganese **(e)**, and phosphate **(f)** at selected L and S stations (the data of major nutrients are from Le Moigne et al., 2012).

However, enhanced Mn concentrations (e.g. 0.8–1.3 nM) were recorded in the upper 100 m at the northern stations close to South Africa (L1 and S1; Figs. 3 and 4). In the ACC the highest surface concentrations were observed on the southern side of the ACC south of PF, particularly at the ACC Southern Boundary (at L7; Fig. 4), whereas comparatively low Mn concentrations occurred in the Weddell Gyre (Fig. 3). Enhanced Mn concentrations in bottom waters were observed above the Mid-Atlantic Ridge (at S4; Figs. 3 and 4).

4 Discussion

4.1 Comparison of datasets of trace metal concentrations obtained at two crossover stations

During the MD166 BONUS-GoodHope cruise, two crossover stations were occupied with the Zero & Drake expedition aboard Polarstern (ANT XXIV/3 cruise; Fahrbach et al., 2011) at about 2 week intervals to allow comparison of trace metals sampling and analyses (Fig. 5). The samples collected during the Zero & Drake expedition were taken using internally Teflon-coated PVC GO-FLO samplers (General Oceanic Inc.) mounted on an all-titanium frame connected to a Kevlar wire (de Baar et al., 2008), as compared to this study, where samples were collected with GO-FLO bottles attached to a Kevlar line and triggered using Teflon-coated messengers. During both cruises, sub-sampling was done after online filtration through 0.2 µM filter cartridges (Sartorius) under pure N_2 pressure, in a class 100 clean room container. The upper 1000 m showed considerable variability in potential temperature at the northern crossover station (e.g. BGH#S2 versus Z&D#101), probably caused by the strong dynamic in this region, and silicate showed offsets of 5–10 % between 1500 and 3000 m at this station (Fig. 5). At the southern crossover station (e.g. BGH#S3 versus Z&D#104), the temperature profiles were very similar, but still an offset of 5–10 % in silicate concentrations was observed in deep waters (Fig. 5). In spite of these differences in hydrology and probably in methodology for silicate analyses, the linear regression

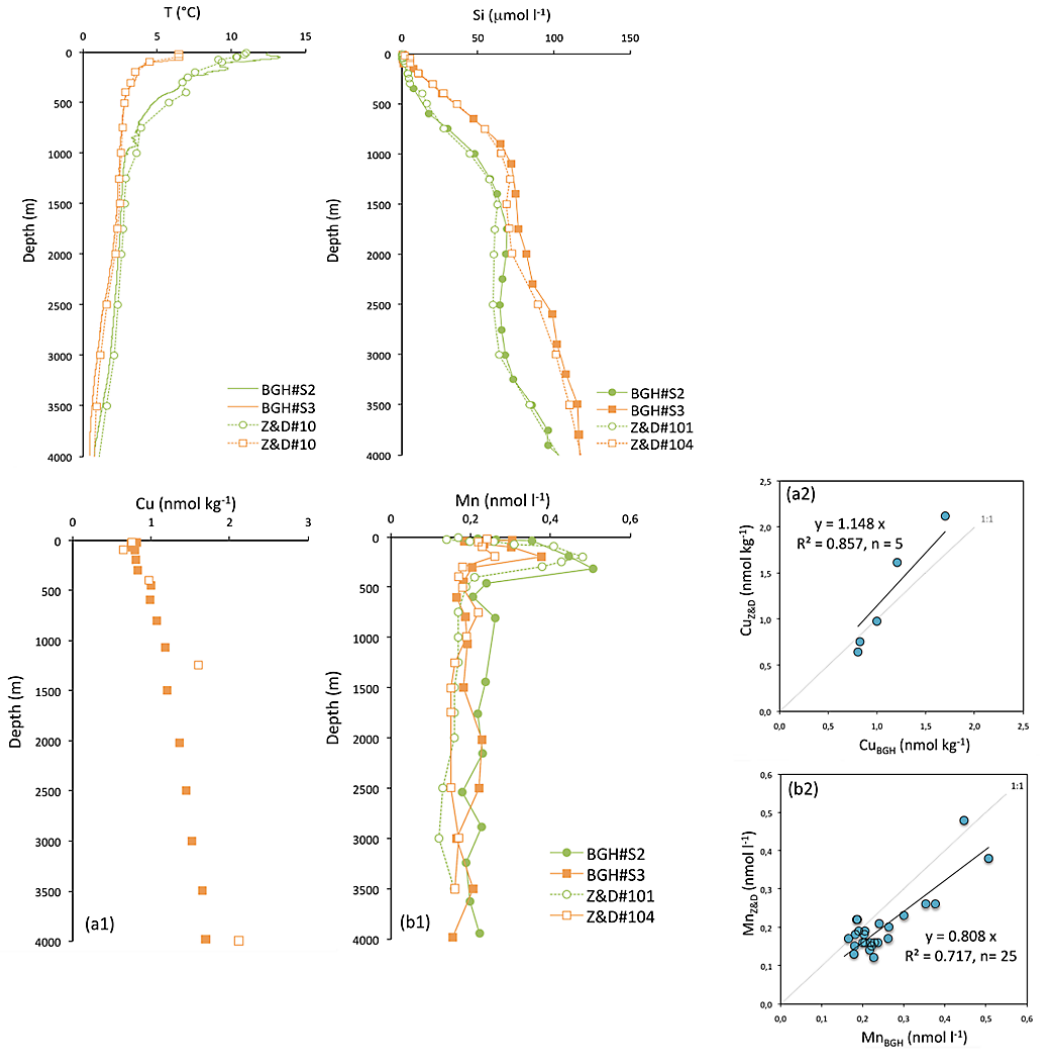

Fig. 5. Comparison of the vertical profiles of temperature (°C) and silicate concentrations (µM) (top panel), and of dissolved copper **(a1)** and manganese **(b1)** concentrations at the two crossover stations of the MD166 BONUS-GoodHope cruise (BGH#S2 at 42.47° S, BGH#S3 at 47.55° S) and the ANT XXIV/3 cruise (Z&D#101 at 42.34° S, Z&D#104 at 47.66° S) along the Greenwhich Meridian. Linear regression between the two datasets of copper concentrations **(a2)** (in nmol kg^{-1}) and of manganese concentrations **(b2)** (in nmol l^{-1}) obtained at the crossover stations (the Z&D dataset of Mn is from Middag et al., 2011a, and of Cu from Heller et al., 2012).

between the two datasets of Cu concentrations is significant ($r^2 = 0.86$, $n = 5$; Fig. 5a2), with the concentrations determined by graphite furnace atomic absorption (ETAAS: Perkin-Elmer Model 4100 ZL) after pre-concentration by simultaneous dithiocarbamate-freon extraction (Heller et al., 2012) being ca. 0.11 nmol kg^{-1} ($n = 5$) higher than those determined by ID-ICPMS (this study), notably in the deep waters below 1000 m (Fig. 5a1). Measurements of the SAFe intercalibration samples S and D2 by graphite furnace atomic absorption yield Cu concentrations of 0.40 ± 0.02 nM ($n = 2$) and 2.22 ± 0.08 nM ($n = 2$), respectively (Heller et al., 2012). These values are lower than consensus values in the surface (Table 1), and in the range of the consensus values in the deep D2 sample (Table 1), again suggesting that the samples may need to be exposed to UV-irradiation prior to analysis (Milne et al., 2010). The comparison of the vertical profiles of Mn generally showed similar shapes at both crossover stations (Fig. 5b1). However, the Mn concentrations determined by ICPMS (this study) yield ca. 0.045 nM ($n = 25$) higher values than those determined by flow-injection analysis and chemiluminescence detection (Middag et al., 2011a) (Fig. 5b2). The factor of 0.808 nM nM^{-1} difference between the ICPMS and FIA-chemiluminescence methods (Fig. 5b2) also falls in the 4 to 9 % offsets of the Mn values we determined by ICPMS in the SAFe *S* and D2 samples compared to the

consensus values (Table 1). Measurements of the SAFe intercalibration samples S and D2 by FIA-chemiluminescence method yield Mn concentrations of 0.73 ± 0.004 nM ($n = 1$) and 0.32 ± 0.01 nM ($n = 37$), respectively (Middag et al., 2011a), in excellent agreement with the consensus values (Table 1); yet, the consensus values are partly dependent on the values reported by Middag et al. (2011a), whereas they are independent of the ones we measured (Table 1). Comparison of two Cd datasets at the southern crossover station showed a good agreement between the isotope dilution thermal ionization mass spectrometry method (O. Baars, personnal communication, 2012) and the ID-ICPMS method (this study) (data not shown). Overall, there is fairly good agreement for Cu and Mn (and Cd) between the two cruises, with some further investigation needed to determine the sources of difference.

4.2 Imprints of the continental margin–open ocean exchanges and external sources

Concentrations of dissolved Pb and Mn in surface waters were the highest close to South Africa where these waters were of Indian Ocean origin (Fig. 3). The waters in this region interact with shelf and slope waters, cyclones and filaments of South Atlantic origin, and are ejected as Agulhas rings from the western boundary current of the South Indian Ocean, the Agulhas Current, at its retroflection (Lutjeharms and Vanballegooyen, 1988). They can be imprinted with external inputs of trace metals from the shelf and slope waters of the South African margin. The waters may also receive atmospheric inputs from Southern Africa-derived sources along their transport route from the Indian Ocean (Piketh et al., 2002). In addition, the Patagonian desert may constitute a dust source (Chever et al., 2010) to the waters west of South Africa. Furthermore, benthic and fluvial sources, such as on the Agulhas Bank, can increase Mn concentrations (Landing and Bruland, 1980; Aguilar-Islas and Bruland, 2006). Atmospheric inputs (Baker et al., 2006), reductive dissolution and subsequent diffusion from sediments above margin and slope (Pakhomova et al., 2007), and photoreduction of Mn oxides in surface waters (Sunda and Huntsman, 1994) also contribute to enhance dissolved Mn concentrations in surface waters. The dry deposition flux of Mn was relatively high in the northernmost part of the section (e.g. ~ 0.8 nmol m^{-2} d^{-1}; Fig. 6), whereas enhanced fluxes were also recorded on the southern side of the ACC (e.g. up to 1.2 nmol m^{-2} d^{-1}; Fig. 6). In addition, Pb has been identified as an excellent tracer for anthropogenic sources of dust and particles to surface waters (Boyle, 2001), and these sources are likely higher on the South African margin than in the remote Southern Ocean. For instance, the highest dry deposition flux of Pb (0.14–0.22 nmol m^{-2} d^{-1}; Fig. 6) was found in the northernmost side of the section. Other trace metals have also shown enrichments in the surface waters close to Africa, such as particulate aluminium (Al) (Jeandel et al., 2010), dissolved cobalt (Co) (Bown et al., 2011), and dissolved and total iron (Fe) (Chever et al., 2010). The isotopic composition of dissolved Fe was also imprinted by the proximity of the African continent in the northern part of the section (Lacan et al., 2008). This further suggests that advection of Indian Ocean waters that interact strongly with shelf and slope waters of the South African margin, as well as with atmospheric inputs and river discharges on the Agulhas Bank, can form a source of trace elements to the southeastern Atlantic Ocean.

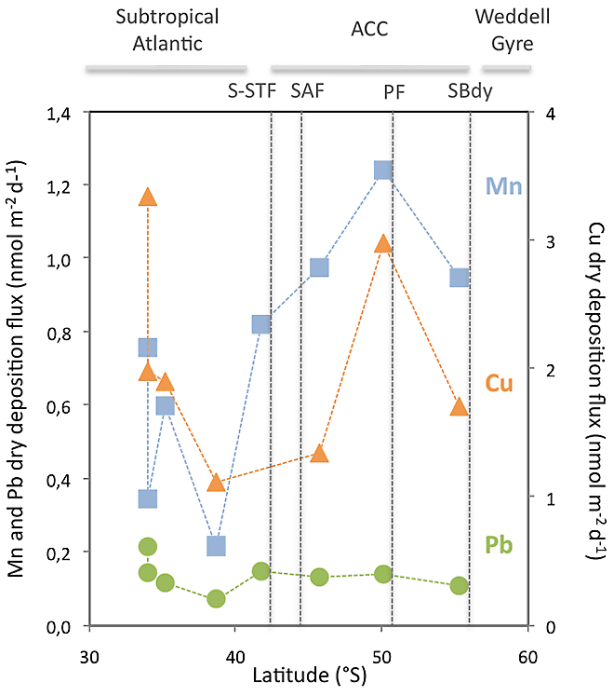

Fig. 6. Dry deposition flux of Mn (blue squares), Cu (orange triangles) and Pb (green circles) (in nmol m^{-2} d^{-1}) as a function of latitude along the section in the southeastern subtropical Atlantic and the Southern Ocean. An estimated dry deposition velocity of 0.3 cm s^{-1} was used to calculate the fluxes.

Ag and Cd dry deposition fluxes were extremely low along the section: from < 0.06 nmol m^{-2} d^{-1} in the northernmost part of the section to < 0.02 nmol m^{-2} d^{-1} in the southern side of the ACC for Ag, and below 0.05 nmol m^{-2} d^{-1} in the northernmost area to < 0.01 nmol m^{-2} d^{-1} in the southern side of the ACC for Cd.

Relatively high concentrations of Cu, Ag, Cd and Mn were also observed in surface waters on the southern side of the ACC, notably at the ACC Southern Boundary, whereas the lowest Pb concentrations were recorded there (Fig. 3). These relatively enhanced concentrations coincided with enhanced dry deposition fluxes of Cu and Mn, which were 1.4 to 2.8 times higher on the southern side of the ACC compared those in the central subtropical domain (Fig. 6), and were observed during snow fall at those latitudes during the expedition. Such snow inputs may have been a source of these trace metals to surface waters at the polar latitudes, which

was further supported by air mass back-trajectories using the NOAA HYSPLIT model (see in Klunder et al., 2011) and independent records of elevated concentrations of Mn (Middag et al., 2011a) and other lithogenic trace metals such as dissolved Co (Bown et al., 2011) and dissolved Al (Middag et al., 2011b). However, the dry deposition can account only for a small fraction of the elevated concentrations of Co (Bown et al., 2011) and Mn (Middag et al., 2011a) at those latitudes. The lateral advection from the Drake Passage in the fast eastwards flowing ACC and the upwelling of enriched Circumpolar Deep Water south of the PF have to be taken into account to explain the enhanced Co and Mn concentrations in these surface waters (Bown et al., 2011; Middag et al., 2011a), and therefore to account for the higher concentrations of the other trace metals. Conversely, the remoteness of anthropogenic sources, as exemplified by the low dry atmospheric Pb flux (0.11–0.14 nmol m^{-2} d^{-1}; Fig. 6) and associated with relative intensification of scavenging processes driven by high export of particles at those latitudes inferred by $^{234}Th/^{238}U$ measurements (Planchon et al., 2012), may have led to the extremely low Pb concentrations at depth.

Shelf-to-open ocean mixing and advection of water masses that have been in contact with continental margins and slopes may well have caused the relative maxima of Pb, Cu and Ag observed in intermediate and deep waters across the section (Fig. 3). For instance, enrichment of these metals in the cores of I-AAIW and A-UCDW may partly reflect sediment and benthic inputs, as well as entrainment of other shelf inputs from the southern margin of South Africa and from the region of formation of A-UCDW in the southwest Atlantic (Whitworth and Nowlin, 1987). Such processes have also been suggested to account for the intermediate and deep relative maxima of particulate Al (Jeandel et al., 2010), dissolved Co (Bown et al., 2011) and dissolved Fe (Chever et al., 2010) along the section. Interestingly, Cu showed a linear correlation with Ag in the water column of the ACC domain of the section ($Ag = 20.61 \cdot Cu + 2.12$ pM nM^{-1}; $r^2 = 0.52$; $n = 81$), which can further support the use of the Ag–Cu relationship as a potential tracer of water masses (Sañudo-Wilhelmy et al., 2002; Ranville and Flegal, 2005). Despite the enrichment of Ag at intermediate depths in the water masses that have been in contact with the continental margin and shelf boundary, its concentrations were relatively depleted in the core of NADW, which had been transported along the southwest African continental shelf or along the continental slope of South America (Fig. 3). Similarly, low dissolved Ag concentrations were recorded in the deep waters of the southeastern Atlantic (Flegal et al., 1995). In fact, it is possible that there is a systematic enrichment of Ag in the deep waters from the North Atlantic towards the North Pacific along the global ocean deep circulation pathway (Zhang et al., 2004). Deep Ag distributions may hence further reflect water mass ages and long-term mixing of deep waters.

In bottom waters there were relatively higher dissolved Mn concentrations (0.30–0.43 nM) over the Bouvet Triple Junction ridge crest at 51.85° S (e.g. station S4; Fig. 3) compared to the other stations at comparable depths (< 0.25 nM). Bottom Mn maxima (> 1 nM) were reported in a dataset of dissolved Mn obtained at higher vertical and horizontal resolutions at the latitudes of 53–54° S, and were deemed to be from hydrothermal inputs (Middag et al., 2011a). The inputs coincided with enhanced concentrations of dissolved Fe (Klunder et al., 2011). It is thus possible that the enhanced deep Mn concentrations we recorded over the Bouvet Triple Junction were due to hydrothermal inputs. However, the strongest feature was missed because of the poor sampling resolution, notably due to the lack of a sampling station in the center of the hydrothermal plume.

4.3 Relationships between Cu, Ag, Mn, Cd and major nutrients in the subtropical Atlantic waters and the Southern Ocean

4.3.1 The silver and silicic acid relationship

Dissolved Ag showed a significant linear relationship with silicic acid (Si) in the water column of the subtropical domain and the Southern Ocean, excluding the data from the Weddell Gyre (Fig. 7a). A good linear correlation between Ag and Si was also reported previously for the Atlantic, with an overall lower Ag / Si ratio (0.11 pM μM^{-1}; Flegal et al., 1995) than observed in our study (e.g. 0.21 pM μM^{-1}; Fig. 7a). A linear relationship was also obtained in the South and equatorial Pacific, with a slope higher than in the Atlantic and much greater concentrations in the surface waters (Zhang et al., 2004). It is thought that the Ag distribution is primarily controlled by uptake by diatoms with subsequent dissolution at depth of biogenic opal (Kramer et al., 2011). However, in the North Pacific Ag and Si were also positively correlated, but the relationship was not linear (Zhang et al., 2004; Kramer et al., 2011), indicating that Ag is not simply incorporated into the siliceous frustule of diatoms (Zhang et al., 2004) and that the ocean Ag cycle may be more complicated. For instance, it has been shown that Ag can be accumulated not only in diatoms but also in dinoflagellates (Fisher and Wente, 1993). Dinoflagellates were abundant in the southernmost subtropical region of the section (Beker and Boye, 2010), and incorporation of Ag in these organisms may have played a role in reducing the surface Ag concentrations (Fig. 3). Furthermore, depletion of Ag relative to silicic acid was observed at intermediate depths in the North Pacific and related to low dissolved oxygen concentrations, with a suggested removal of Ag by scavenging and/or precipitation with sulfides that may account for the curvature in the Ag–Si relationship (Kramer et al., 2011; Zhang et al., 2004). Relative minima of Ag were observed in the oxygen-depleted zone in our study (Fig. 3). However, the oxygen concentration in this part of the water column was relatively high along the section across the subtropical southeast Atlantic (e.g. > 230 µM) and the Southern Ocean (e.g. > 170 µM) compared with the North Pacific

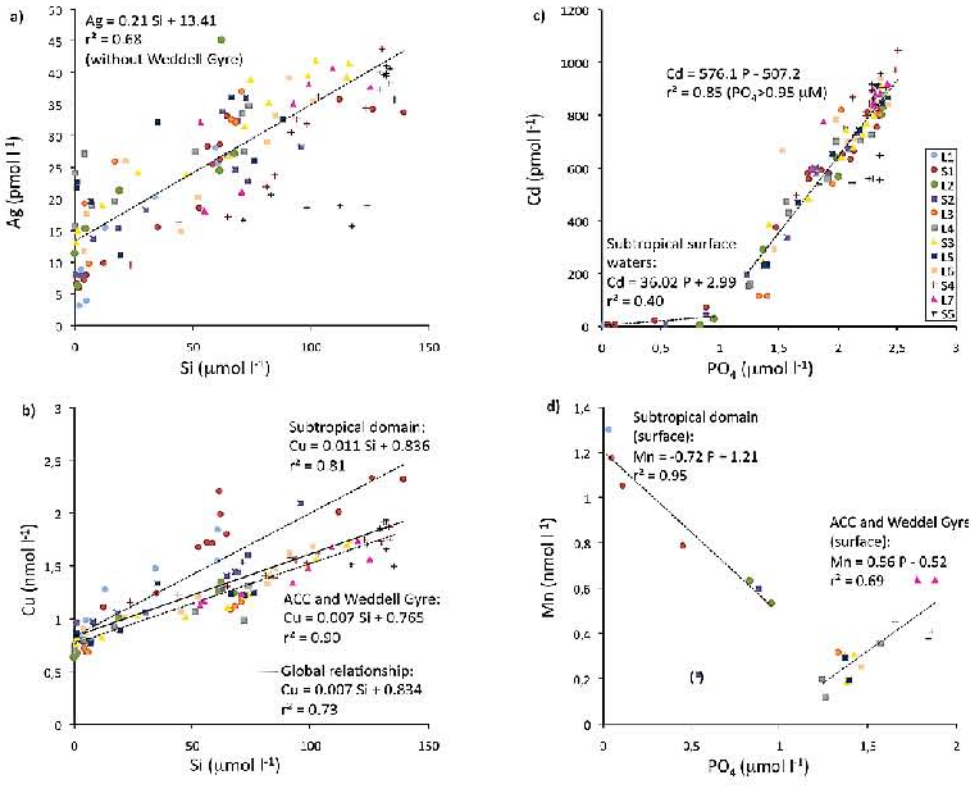

Fig. 7. Relationships among the concentrations of Ag (in pM) **(a)**, Cu (in nM) **(b)** and silicic acid (Si; in µM); and Cd (in pM) **(c)**, Mn (in nM) **(d)** and phosphate (PO_4; in µM) along the section between the southeastern Atlantic and the Southern Ocean. The coloured symbols stand for each station.

(e.g. 150 µM; Kramer et al., 2011), potentially leading to a minor removal of Ag in those waters.

4.3.2 The copper and silicic acid relationship

Dissolved Cu showed a strong linear correlation with Si in the water column across the section, with a slightly lower Cu / Si ratio in the ACC and Weddell Gyre (e.g. 0.007 nM µM^{-1}) than in the subtropical waters (e.g. 0.011 nM µM^{-1}; Fig. 7b). Strong linear relationships between Cu and Si were previously observed in the Atlantic sector of the Southern Ocean with higher Cu / Si ratios (e.g. 0.013–0.018 nM g µM^{-1}) in the relatively productive Polar Frontal region during spring (Löscher, 1999), compared to those in the diatom post-bloom area centered on the Polar Front (e.g. 0.004 nM µM^{-1}) during our late summer expedition (Le Moigne et al., 2012). The seasonal decrease of the Cu / Si ratio over the diatom productive season is probably due to preferential Si uptake by diatoms in the upper water column and Cu scavenging in deeper waters, as well as to a longer retention of Cu compared to Si during dissolution of the diatom frustules in the sediments (Löscher, 1999). The decrease in Cu / Si ratio in the Polar Frontal region over the productive season also coincided with a decrease of Cu concentrations in surface waters from about 1.5 nM (Löscher, 1999) to about 0.9 nM (this study, station L6; Fig. 3). In a section across the Subantarctic zone in the Australian sector of the Southern Ocean, the decrease in Cu concentrations between summer and winter conditions was less pronounced (e.g. 0.1–0.2 nM), and was correlated with a drawdown of PO_4 by about 0.4 µM (Ellwood, 2008). The low Cu / Si ratio and the relative depletion of Cu observed in the vast post-diatom bloom area centered on the Polar Front coincided with depletion of dissolved Fe in the surface waters (< 0.25 nM; Chever et al., 2010). The relative low concentrations of both Cu and Fe in these surface waters indicate an involvement of Cu in the Fe uptake process of oceanic diatoms (Maldonado et al., 2006). The relationship between the uptake of Cu and Fe by diatoms could not be observed in the HNLC surface waters where Cu concentrations increased southwards (Fig. 3), in contrast to Fe (Chever et al., 2010). Differences in biogeochemical cycling of Fe and Cu, especially due to external sources and mixed layer recycling processes, as well as particle reactivity may cause the different trends observed in surface waters of the HNLC area. The Cu / Si depletion ratio was slightly higher in the subtropical waters than in the ACC and Weddell Gyre, where the ratios were similar to the global relationship obtained along the section (Fig. 7b). The strongest removal of Cu was observed in the southernmost subtropical region

(Fig. 3), where nanoflagellates dominated the phytoplankton assemblage and dinoflagellates were also abundant (Beker and Boye, 2010). Dinoflagellates and nanoflagellates, such as prasinophyceae, have a relatively higher Cu cellular quota compared to diatoms (Ho et al., 2003). Hence, this observation suggests that other taxa than diatoms are able to control the removal of Cu from the surface waters such as in the southeastern Atlantic Ocean, and therefore the Cu / Si ratio.

4.3.3 The cadmium and phosphate relationship

Cadmium correlated strongly with phosphate (P), at phosphate concentrations above 0.95 µM. In the subtropical surface waters, phosphate concentrations were below 0.95 µM, yielding a very low Cd / P ratio (Fig. 7c) as cadmium was strongly depleted (Fig. 3). Earlier work showed this "kink" to occur at phosphate concentrations of less than 1.3 µM, which accounted for surface and most of deep North Atlantic waters (Boyle, 1988). Recently, a similar trend has been observed in the southern subtropical and the subantarctic regions of the Australian sector, but at the phosphate concentration boundary of 0.74 µM (Ellwood, 2008). The reasons for the much lower Cd / P ratio in the subtropical surface waters compared with the Southern Ocean may be related to lower inputs of both Cd and P to subtropical waters, and to differences in Cd / P cellular ratios due to differences in the species composition of the phytoplankton community. The nanoflagellates and dinoflagellates, which dominated in the subtropical domain, have higher reported Cd / P ratios than the diatoms which were blooming in the Polar Frontal Zone (Ho et al., 2003). In the Southern Ocean there was also a "kink" in the Cd–P relationship with a greater depletion of Cd relative to P in the southernmost surface waters, due to the decrease of Cd concentrations in the Weddell Gyre compared to those in the southern ACC (Fig. 8). A similar trend of a southward enhanced depletion of Cd relative to P across the Southern Boundary of the ACC and in the Weddell Gyre was observed along the Greenwich Meridian (Abouchami et al., 2011). The stronger depletion of Cd relative to P in nutrient-rich Antarctic surface waters may result from the increase of the Cd uptake rate induced by the extremely low dissolved Fe concentrations recorded in those waters (< 0.11 nM; Chever et al., 2010). Under Fe-limiting conditions, phytoplankton have been shown to take up more Cd than under Fe-replete conditions (Sunda and Huntsman, 2000; Cullen et al., 2003; Cullen, 2006). In addition, culture experiments have indicated that there are two transport systems of Cd in marine diatoms, a low-zinc (Zn) induced system and a Mn-uptake system at high-Zn concentrations (Sunda and Huntsman, 1998). The Mn-uptake system furthermore strengthens as the Mn concentration decreases (Sunda and Huntsman, 1998). An increase of Cd uptake via Mn transporters in the Weddell Gyre, and thus a relative depletion of Cd concentrations, can thus be related to lower dissolved Mn concentrations (Fig. 3) along with higher dissolved Zn concentrations (Croot et al., 2011) in the Weddell Gyre compared to those in the ACC. A shift from a predominant Mn system of Cd uptake in the Weddell Gyre to the low-Zn system in the ACC has been recently suggested to explain the increase in magnitude of the Cd isotope fractionation factor from the Weddell Gyre into the ACC (Abouchami et al., 2011).

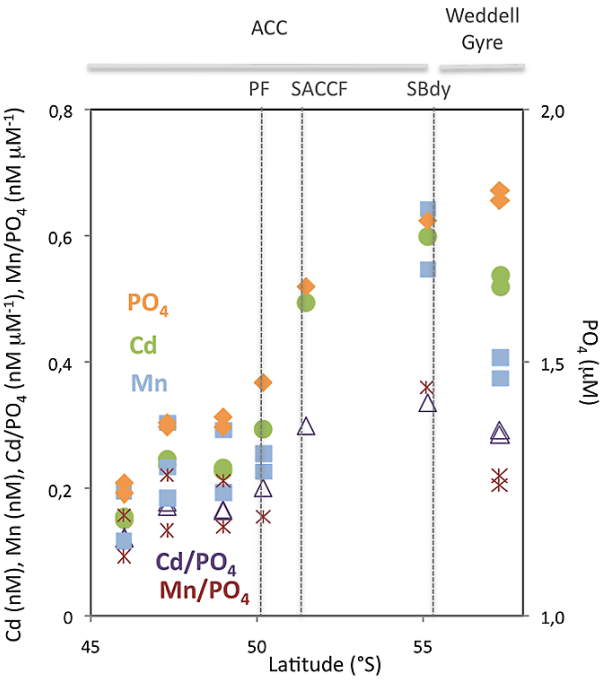

Fig. 8. Variations of Cd (green circles, in nM), Mn (blue squares, in nM) and PO_4(orange diamonds, in µM) concentrations, and of Cd / PO_4 (purple triangles) and Mn / PO_4 (dark red crosses) ratios (in nM g μM^{-1}) as a function of latitude in the surface waters (> 60 m) of the Antarctic Circumpolar Current and the northern Weddell Gyre along the Greenwich Meridian.

4.3.4 The manganese and phosphate relationship

A strong linear relationship with a negative slope was observed between dissolved Mn and P in the subtropical surface waters (Fig. 7d). High inputs of Mn in the northernmost surface waters from advection of enriched waters transported off the South African margin, as well as atmospheric inputs (Fig. 6) and photo-reduction of Mn oxides in surface waters probably caused the trend of a southward decrease of Mn concentrations in the surface subtropical waters (Fig. 3). Inversely, phosphate concentrations increased southward in these waters (Le Moigne et al., 2012). The opposite gradients of Mn and P concentrations hence caused the negative Mn–P relationship recorded in these waters. In the ACC and the Weddell Gyre, dissolved Mn correlated positively with P in the surface waters (Fig. 7d). Similar Mn–P relationships were recently observed in the Atlantic sector of the Southern Ocean, but with lower Mn / P ratios

(e.g. 0.36 nM μM^{-1} in the surface ACC, and 0.39 nM μM^{-1} in the surface Weddell Gyre; Middag et al., 2011a) compared to the value in this work obtained at a lower spatial resolution and without the exclusion of the highest Mn values at the ACC Southern Boundary (e.g. 0.56 nM μM^{-1}; Fig. 7d). The mean Mn / P depletion ratio observed in the surface waters of the ACC and northeastern side of the Weddell Gyre (e.g. 0.56 nM μM^{-1}) was in the range of elemental ratio in diatoms (0.42 nM μM^{-1}; Twining et al., 2004) and of the elemental ratio measured with bulk analysis of natural phytoplankton assemblages from the Southern Ocean (1.68 nM μM^{-1}; Cullen et al., 2003), but somewhat higher than the Redfield ratio ($\sim$ 0.4 nM μM^{-1}; Bruland et al., 1991). Furthermore, there was a greater depletion of Mn relative to P in the southernmost surface waters beyond the ACC Southern Boundary, as seen for Cd, due to lower Mn concentrations in the Weddell Gyre compared to those in the southern ACC (Fig. 8). This feature was not directly apparent in the global relationship obtained for surface waters of the Southern Ocean (Fig. 7d), due to the limited dataset for the Weddell Gyre. Nevertheless, the increase in Mn uptake in the Weddell Gyre was further supported by a lower slope in the Mn–P relationship in the Weddell Gyre along the Greenwich Meridian compared to the higher slope obtained in the ACC waters (Middag et al., 2011a). An increase of the Mn requirement by diatoms under Fe-depleted conditions (Peers and Price, 2004) can cause the increase of Mn uptake rate and consequently the highest depletion of Mn relative to P in the surface waters of the Weddell Gyre, since extremely low dissolved Fe concentrations were recorded in these waters (<0.11 nM; Chever et al., 2010). In addition, the cellular Mn-transport channel of Cd (Sunda and Huntsman, 1998) was possibly activated in the Weddell Gyre, since dissolved Zn concentrations were higher there compared to the concentrations in the ACC (Croot et al., 2011). In turn, the higher uptake rate of Mn due to low Fe conditions and the induction of a Mn-uptake system may have caused a greater depletion of Mn relative to P in the Weddell Gyre.

5 Conclusions

The advection of water masses enriched in trace metals following contact with continental margins can be an important source of trace elements to the surface and intermediate waters of the southeast Atlantic Ocean. South African margins have been identified as a source of trace metals to the subtropical Atlantic, in addition to atmospheric deposition. Furthermore, transport of trace elements from source regions in the Drake Passage and southwestern Atlantic in the fast eastward-flowing jet of the ACC forms a pathway to the Greenwich Meridian. Synoptic analyses of trace elements, as first assessed in this work, and of isotopes will further help to identify the external sources of trace metals to our study region and allow us to understand the boundary exchange processes that determine the oceanic budget of trace metals (Lacan and Jeandel, 2001). In addition, hydrothermal inputs above the Mid-Atlantic Ridge can also be a source of trace elements like Mn, and deserve further investigation. Hydrothermal vents can significantly contribute to the trace elements inventory in the ocean, as suggested for dissolved Fe (Tagliabue et al., 2010). The strong and different relationships between trace elements and major nutrients in the different biogeochemical domains of the subtropical Atlantic, the ACC and the Weddell Gyre illustrated the variety of biological requirements of trace metals by the different phytoplankton assemblages. It also indicated that the biogeochemical cycles of these trace elements can be connected in the water column through their capability of activating or substituting in the phytoplankton uptake systems. The metal interplays can be an important adaptation to life in ocean surface waters where these trace nutrients are often depleted (Saito et al., 2010). Synoptic records of various trace nutrients will further help in revealing their specific and tight couplings in phytoplankton growth, productivity and diversity.

Supplementary material related to this article is available online at: http://www.biogeosciences.net/9/3231/2012/bg-9-3231-2012-supplement.pdf.

Acknowledgements. We gratefully acknowledge the Captain P. Courtes, the officers and crew members of the French *R/V Marion Dufresne II* for their wonderful work at sea during the MD166 BONUS-GoodHope cruise. H. Leau and P. Sangiardi (IPEV, France) are also thanked for their logistical and technical support during the operations at sea. M. Boye extends special thanks to S. Speich (LPO, France) for her partnership in the coordination of the BONUS-GoodHope project and cruise; and to collaborators M. Arhan (LPO, France) and F. Dehairs (VUB, Belgium) for their help and advices in conducting the scientific strategy during the cruise. This investigation was supported by the French LEFE National Program of Institut des Sciences de l'Univers du Centre National de la Recherche Scientifique (INSU-CNRS), the National Agency for Research Funding (ANR-07-BLAN-0146), IFREMER and the French Polar Institut (IPEV). We acknowledge the GO-FLO sampling team: F. Chever, E. Bucciarelli, F. Lacan, G. Sarthou, A. Radic. Thanks to Patrick Laan and J. Andy Milton for assistance in analysis, and Angie Milne and Bill Landing for their help with setting up the ID-ICPMS technique. Special thanks to our fellows from the NIOZ team led by H. de Baar on board of the *R/V Polarstern* for synoptic work and extension of the section towards Antarctica along the Greenwich Meridian during the International Polar Year. The Postdoctoral Fellowship of B. W. was supported by the Network of Excellence EUR-OCEANS, the ANR-07-BLAN-0146 project and the University of Southampton. Ph.D. fellowship of J. B. was supported by the Région Bretagne. This work is a contribution to the International Polar Year and GEOTRACES programs.

Edited by: F. Dehairs

The publication of this article is financed by CNRS-INSU.

References

Abouchami, W., Galer, S. J. G., de Baar, H. J. W., Alderkamp, A. C., Middag, R., Laan, P., Feldmann, H., and Andreae, M. O.: Modulation of the Southern Ocean cadmium isotope signature by ocean circulation and primary productivity, Earth Planet. Sci. Lett., 305, 83–91, 2011.

Aguilar-Islas, A. M. and Bruland, K. W.: Dissolved manganese and silicic acid in the Columbia River plume: a major source to the California current and coastal waters off Washington and Oregon, Mar. Chem., 101, 233–247, 2006.

Arhan, M., Mercier, H., and Park, Y. H.: On the deep water circulation of the eastern South Atlantic Ocean, Deep-Sea Res. Pt. I, 50, 889–916, 2003.

Baker, A. R., Jickells, T. D., Witt, M., and Linge, K. L.: Trends in the solubility of iron, aluminium, manganese and phosphorus in aerosol collected over the Atlantic Ocean, Mar. Chem., 98, 43–58, 2006.

Baker, A. R., Weston, K., Kelly, S. D., Voss, M., Streu, P., and Cape, J. N.: Dry and wet deposition of nutrients from the tropical Atlantic atmosphere: links to primary productivity and nitrogen fixation, Deep-Sea Res. Pt. I, 54, 1704–1720, 2007.

Baker, A. R., Lesworth, T., Adams, C., Jickells, T. D., and, Ganzeveld, L.: Estimation of atmospheric nutrient inputs to the Atlantic Ocean from 50° N to 50° S based on large-scale field sampling: Fixed nitrogen and dry deposition of phosphorus, Global Biogeochem. Cy., 24, GB3006, doi:10.1029/2009GB003634, 2010.

Barriada, J. L., Tappin, A. D., Evans, E. H., and Achterberg, E. P.: Dissolved silver measurements in seawater, Trac-Trend. Anal. Chem., 26, 809–817, 2007.

Beker, B. and Boye, M.: Phytoplankton assemblages in the Southern Ocean during the International Polar Year, AGU OS10 Scientific Program, Ocean Sciences Conference (AGU/ASLO), Portland, USA, 2010.

Boebel, O., Lutjeharms, J., Schmid, C., Zenk, W., Rossby, T., and Barron, C.: The Cape Cauldron: a regime of turbulent inter-ocean exchange, Deep-Sea Res. Pt. II, 50, 57–86, 2003.

Bown, J., Boye, M., Baker, A., Duvieilbourg, E., Lacan, F., Le Moigne, F., Planchon, F., Speich, S., and Nelson, D. M.: The biogeochemical cycle of dissolved cobalt in the Atlantic and the Southern Ocean south off the coast of South Africa, Mar. Chem., 126, 193–206, 2011.

Boyd, P. W., Jickells, T., Law, C. S., Blain, S., Boyle, E. A., Buesseler, K. O., Coale, K. H., Cullen, J. J., de Baar, H. J. W., Follows, M., Harvey, M., Lancelot, C., Levasseur, M., Owens, N. P. J., Pollard, R., Rivkin, R. B., Sarmiento, J., Schoemann, V., Smetacek, V., Takeda, S., Tsuda, A., Turner, S., and Watson, A. J.: Mesoscale iron enrichment experiments 1993–2005: Synthesis and future directions, Science, 315, 612–617, 2007.

Boyle, E. A.: Cadmium: chemical tracer of deepwater paleoceanography, Paleoceanography, 3, 471–489, 1988.

Boyle, E. A.: Anthropogenic trace elements in the ocean, in: Encyclopedia of Ocean Sciences, edited by: Steele, J. H. and Turekain, K. K., Academic Press, 162–169, 2001.

Boyle, E. and Edmond, J. M.: Copper in surface waters south of New Zealand, Nature, 253, 107–109, 1975.

Branellec, P., Arhan, M., and Speich, S.: Projet GoodHope, campagne Bonus-GoodHope, rapport de données CTD-O_2, Rapport interne OPS/LPO 10-02, IFREMER Edition, 2010.

Bruland, K. W. and Lohan, M. C.: Controls of Trace Metals in Seawater, Treatise on Geochemistry, edited by: Elderfield, H., Elsevier Science Ltd., Cambridge, 2003.

Bruland, K. W., Donat, J. R., and Hutchins, D. A.: Interactive influences of bioactive trace-metals on biological production in oceanic waters, Limnol. Oceanogr., 36, 1555–1577, 1991.

Chever, F., Bucciarelli, E., Sarthou, G., Speich, S., Arhan, M., Penven, P., and Tagliabue, A.: Physical speciation of iron in the Atlantic sector of the Southern Ocean, along a transect from the subtropical domain to the Weddell Sea Gyre, J. Geophys. Res. Ocean, 115, C10059, doi:10.1029/2009JC005880, 2010.

Croot, P. L., Baars, O., and Streu, P.: The distribution of dissolved zinc in the Atlantic sector of the Southern Ocean, Deep-Sea Res. Pt. II, 58, 2707–2719, 2011.

Cullen, J. T.: On the nonlinear relationship between dissolved cadmium and phosphate in the modern global ocean: could chronic iron limitation of phytoplankton growth cause the kink?, Limnol. Oceanogr., 51, 1369–1380, 2006.

Cullen, J. T., Chase, Z., Coale, K. H., Fitzwater, S. E., and Sherrell, R. M.: Effect of iron limitation on the cadmium to phosphorus ratio of natural phytoplankton assemblages from the Southern Ocean, Limnol. Oceanogr., 48, 1079–1087, 2003.

de Baar, H. J. W., Saager, P. M., Nolting, R. F., and van der Meer, J.: Cadmium versus phosphate in the world ocean, Mar. Chem., 46, 261–281, 1994.

de Baar, H. J. W., Boyd, P. W., Coale, K. H., Landry, M. R., Tsuda, A., Assmy, P., Bakker, D. C. E., Bozec, Y., Barber, R. T., Brzezinski, M. A., Buesseler, K. O., Boye, M., Croot, P. L., Gervais, F., Gorbunov, M. Y., Harrison, P. J., Hiscock, W. T., Laan, P., Lancelot, C., Law, C. S., Levasseur, M., Marchetti, A., Millero, F. J., Nishioka, J., Nojiri, Y., van Oijen, T., Riebesell, U., Rijkenberg, M. J. A., Saito, H., Takeda, S., Timmermans, K. R., Veldhuis, M. J. W., Waite, A. M., and Wong, C.-S.: Synthesis of iron fertilization experiments: from the Iron Age in the Age of Enlightenment, J. Geophysical Res.-Ocean., 110, 1–24, 2005.

de Baar, H. J. W., Timmermans, K. R., Laan, P., De Porto, H. H., Ober, S., Blom, J. J., Bakker, M. C., Schilling, J., Sarthou, G., Smit, M. G., and Klunder, M.: Titan: A new facility for ultraclean sampling of trace elements and isotopes in the deep oceans in the international Geotraces program, Mar. Chem., 111, 4–21, 2008.

Duce, R. A., Liss, P. S., Merrill, J. T., Atlas, E. L., Buat-Menard, P., Hicks, B. B., Miller, J. M., Prospero, J. M., Arimoto, R., Church, T. M., Ellis, W., Galloway, J. N., Hansen, L., Jickells, T. D., Knap, A. H., Reinhardt, K. H., Schneider, B., Soudine, A., Tokos, J. J., Tsunogai, S., Wollast, R., and Zhou, M.: The atmospheric input of trace species to the world ocean, Global Biogeochem. Cy., 5, 193–259, 1991.

Elderfield, H. and Rickaby, R. E. M.: Oceanic Cd / P ratio and nutrient utilization in the glacial Southern Ocean, Nature, 405, 305–

310, 2000.

Ellwood, M. J.: Wintertime trace metal (Zn, Cu, Ni, Cd, Pb and Co) and nutrient distributions in the Subantarctic Zone between 40–52° S; 155–160° E, Mar. Chem., 112, 107–117, 2008.

Fahrbach, E., de Baar, H. J. W., Garçon, V. C., and Provost, C.: Introduction to physics, carbon dioxide, trace elements and isotopes in the Southern Ocean: The Polarstern expeditions ANT-XXIV/3 (2008) and ANT-XXIII/3 (2006), Deep-Sea Res. Pt. II, 58, 2501–2508, 2011.

Fisher, N. S. and Wente, M.: The release of trace elements by dying marine phytoplankton, Deep-Sea Res. Pt. I, 40, 671–694, 1993.

Flegal, A. R. and Patterson, C. C.: Vertical concentration profiles of lead in the Central Pacific at 15° N and 20° S, Earth Planet. Sci. Lett., 64, 19–32, 1983.

Flegal, A. R., Sañudo-Wilhelmy, S. A., and Scelfo, G. M.: Silver in the eastern Atlantic Ocean, Mar. Chem., 49, 315–320, 1995.

Gladyshev, S., Arhan, M., Sokov, A., and Speich, S.: A hydrographic section from South Africa to the southern limit of the Antarctic Circumpolar Current at the Greenwich meridian, Deep-Sea Res. Pt. I, 55, 1284–1303, 2008.

Gordon, A. L., Weiss, R. F., Smethie, W. M., and Warner, M. J.: Thermocline and Intermediate Water Communication between the South-Atlantic and Indian Oceans, J. Geophys. Res.-Ocean., 97, 7223–7240, 1992.

Heller, M. I., et al.: Copper speciation and distribution in the Weddell Sea and Drake Passage, Deep-Sea Res. Pt. I., in prep., 2012.

Ho, T.-Y., Quigg, A., Finkel, Z. V., Milligan, A. J., Wyman, K., Falkowski, P. G., and Morel, F. M. M.: The elemental composition of some marine phytoplankton, J. Phycol., 39, 1145–1159, 2003.

Jeandel, C., Lacan, F., and Labatut, M.: Trace element concentrations of the suspended particles in the Southern Ocean (Bonus/GoodHope transect), AGU OS10 Scientific Program, Ocean Sciences Conference (AGU/ASLO), Portland, USA, 2010.

Kermabon, C. and Arhan, M.: SBE9+: validation et réduction des données, Rapport interne OPS/LPO 08-04, IFREMER Edition, 2008.

Klunder, M., Laan, P., Middag, R., de Baar, H. J. W., and van Ooijen, J. C.: Distributions and sources of dissolved iron over a prime meridian transect in the Southern Ocean, Deep-Sea Res. Pt. II, 58, 2678–2694, 2011.

Kramer, D., Cullen, J.T., Christian, J.R., Johnson, W.K., and Pedersen, T.F.: Silver in the subarctic northeast Pacific Ocean: explaining the basin scale distribution of silver, Mar. Chem., 123, 133–142, 2011.

Lacan F. and Jeandel C.: Tracing Papua New Guinea imprint on the central Equatorial Pacific Ocean using neodymium isotopic compositions and Rare Earth Element patterns, Earth Planet. Sci. Lett., 186, 497–512, 2001.

Lacan, F., Radic, A., Jeandel, C., Poitrasson, F., Sarthou, G., Pradoux, C., and Freydier, R.: Measurement of the isotopic composition of dissolved iron in the open ocean, Geophys. Res. Lett., 35, L24610, doi:10.1029/2008GL035841, 2008.

Landing, W. M. and Bruland, K. W.: Manganese in the North Pacific, Earth Planet. Sci. Lett., 49, 45–56, 1980.

Le Moigne, F. A. C., Boye, M., Masson, A., Corvaisier, R., Grossteffan, E., Guéneugues, A., and Pondaven, P.: Description of the biogeochemical features of the subtropical southeastern Atlantic and the Southern Ocean south off South Africa during the austral summer of the International Polar Year, Biogeosciences Discuss., 9, 5011–5048, doi:10.5194/bgd-9-5011-2012, 2012.

Löscher, B. M.: Relationships among Ni, Cu, Zn, and major nutrients in the Southern Ocean, Mar. Chem., 67, 67–102, 1999.

Lutjeharms, J. R. E. and Vanballegooyen, R. C.: The Retroflection of the Agulhas Current, J. Phys. Oceanogr., 18, 1570–1583, 1988.

Maldonado, M. T., Allen, A. E., Chong, J. S., Lin, K., Leus, D., Karpenko, N., and Harris, S. L.: Copper-dependent iron transport system in coastal and oceanic diatoms, Limnol. Oceanogr., 51, 1729–1743, 2006.

Martin, J. H., Gordon, R. M., and Fitzwater, S. E.: Iron in Antarctic waters, Nature, 345, 156–158, 1990.

Meredith, M., Locarnini, R., Van Scoy, K., Watson, A., Heywood, K., and King B.: On the sources of Weddell Gyre Antarctic Bottom Water, J. Geophys. Res., 105, 1093–1104, doi:10.1029/1999JC900263, 2000.

Middag, R., de Baar, H. J. W., Laan, P., Cai, P. H., and van Ooijen, J. C.: Dissolved manganese in the Atlantic sector of the Southern Ocean, Deep-Sea Res. Pt. II, 58, 2661–2667, 2011a.

Middag, R., van Slooten, C., de Baar, H. J. W., and Laan, P.: Dissolved aluminium in the Southern Ocean, Deep-Sea Res. Pt. II, 58, 2647–2660, 2011b.

Milne, A., Landing, W., Bizimisb, M., and Mortona, P.: Determination of Mn, Fe, Co, Ni, Cu, Zn, Cd and Pb in seawater using high resolution magnetic sector inductively coupled mass spectrometry (HR-ICP-MS), Anal. Chim. Acta, 665, 200–207, 2010.

Orsi, A. H., Nowlin, W. D., and Whitworth III, T.: On the circulation and stratification of the Weddell Gyre, Deep-Sea Res. Pt. I, 40, 169–203, 1993.

Pakhomova, S. V., Hall, P. O. J., Kononets, M. Yu., Rozanov, A. G., Tengberg, A., and Vershinin, A. V.: Fluxes of iron and manganese across the sediment-water interface under various redox conditions, Mar. Chem., 107, 319–331, 2007.

Peers, G. and Price, N. M.: A role for manganese in superoxide dismutases and growth of iron-deficient diatoms, Limnol. Oceanogr., 49, 1774–1783, 2004.

Piketh, S., Swap, R., Maenhaut, W., Annegarn, H., and Formenti, P.: Chemical evidence of long-range atmospheric transport over southern Africa, J. Geophys. Res., 107, 4817, doi:10.1029/2002JD002056, 2002.

Piola, A. R. and Gordon, A. L.: Intermediate Waters in the Southwest South-Atlantic, Deep-Sea Res., 36, 1–16, 1989.

Planchon, F., Cavagna, A.-J., Cardinal, D., André, L., Dehairs,, F.: Late summer particulate organic carbon export and twilight zone remineralisation in the Atlantic sector of the Southern Ocean, Biogeosciences Discuss., 9, 3423–3477, doi:10.5194/bgd-9-3423-2012, 2012.

Ranville, M. A. and Flegal, A. R.: Silver in the North Pacific Ocean, Geochem. Geophy. Geosy., 6, Q03M01, doi:10.1029/2004GC000770, 2005.

Rickli, J., Frank, M., Baker, A. R., Aciego, S., de Souza, G., Georg, R. B., and Halliday, A. N.: Hafnium and neodymium isotope distribution in surface waters of the eastern Atlantic Ocean: Implications for sources and inputs of trace metals to the ocean, Geochim. Cosmochim. Ac., 74, 540–557, doi:10.1016/j.gca.2009.10.006, 2010.

Saito, M. A., Goepfert, T. J., Noble, A. E., Bertrand, E. M., Sedwick, P. N., and DiTullio, G. R.: A seasonal study of dissolved cobalt in the Ross Sea, Antarctica: micronutrient behavior, absence of scavenging, and relationships with Zn, Cd, and P, Biogeosciences, 7, 4059–4082, doi:10.5194/bg-7-4059-2010, 2010.

Sañudo-Wilhelmy, S. A., Olsen, K. A., Scelfo, J. M., Foster, T. D., and Flegal, A. R.: Trace metal distribution off the Antarctic Peninsula in the Weddell Sea, Mar. Chem., 77, 157–170, 2002.

Schlitzer, R.: Ocean Data View, http://odv.awi.de, 2012.

Sunda, W. G. and Huntsman, S. A.: Photoreduction of manganese oxides in seawater, Mar. Chem., 61, 133–152, 1994.

Sunda, W. G. and Huntsman, S. A.: Processes regulating cellular metal accumulation and physiological effects: phytoplankton as model systems, Sci. Total Environ., 219, 165–181, 1998.

Sunda, W. G. and Huntsman, S. A.: Effect of Zn, Mn, and Fe on Cd accumulation in phytoplankton: Implications for oceanic Cd cycling, Limnol. Oceanogr., 45, 1501–1516, 2000.

Tagliabue, A., Bopp, L., Dutay, J.-C., Bowie, A. R., Chever, F., Jean-Baptiste, P., Bucciarelli, E., Lannuzel, D., Remenyi, T., Sarthou, G., Aumont, O., Gehlen, M., and Jeandel, C.: Hydrothermal contribution to the oceanic dissolved iron inventory, Nat. Geosci., 3, 252–256, 2010.

Twining, B. S., Baines, S. B., and Fisher, N. S.: Elemental stoichiometries of individual plankton cells collected during the Southern Ocean Iron Experiment (SOFEX), Limnol. Oceanogr., 49, 2115–2128, 2004.

Whitworth, T. and Nowlin, W. D.: Water masses and currents of the Southern Ocean at the Greenwich meridian, J. Geophys. Res.-Ocean., 92, 6462–6476, 1987.

Xie, P. and Arkin, P. A.: Global Precipitation: A 17-Year Monthly Analysis Based on Gauge Observations, Satellite Estimates, and Numerical Model Outputs, B. Am. Meteorol. Soc., 78, 2539–2558, 1997.

Yang, L. and Sturgeon, R. E.: On-line determination of silver in sea-water and marine sediment by inductively coupled plasma mass spectrometry, J. Anal. Atom. Spectrom., 17, 88–93, doi:10.1039/B109409M, 2002.

Zhang, Y., Obata, H., and Nozaki, Y.: Silver in the Pacific Ocean and the Bering Sea, Geochem. J., 38, 623–633, 2004.